Defect Analysis with TCAD-based DLTS Simulation

A. Scheinemann and A. Schenk
Integrated Systems Laboratory, ETH Zürich, Gloriastrasse 35, 8092 Zürich, Switzerland
e-mail: scheinemann@iis.ee.ethz.ch

Introduction

Although DLTS [1] is a wide-spread characterization technique and has been studied quite extensively, its key properties have to be reconsidered when facing the characterization of extended defects which are often observed in todays CMOS processes. In most cases the characterized samples contain more than one defect level. Hence, the measured capacitance transients are not single time constant exponential functions but superpositions of different decay processes in the form of $C(t) = \sum_{i=1}^{n} C_i(0)e^{-e_i t}$ where n is the number of different species and e_i is the emission rate containing the most important physical parameters of the defect. Furthermore, the spatial defect distributions in general cannot be assumed homogeneous, e.g. in the case of end-of-range (EOR) defects introduced during amorphising implants. This renders the use and fitting of analytical expressions to measured DLTS signals not applicable.

Methodology

Experiments on dedicated samples for the study of extended defects exhibit a multitude of different defect species some of which appear to be strongly broadened. In the majority of available literature DLTS peaks are compared to the analytical expression

$$S(T) = C_{\mathrm{Trap}}(e^{-e_\nu(T,E_T,\sigma_\nu)t_1} - e^{-e_\nu(T,E_T,\sigma_\nu)t_2}) \ , \quad (1)$$

where C_{Trap} denotes the capacitance difference between filled and empty defects and e_ν with $\nu \in \{n, p\}$is the emission rate which couples the defect levels to the corresponding carrier band. This signal as it results from the original box car DLTS method introduced by Lang [1] as well as many other approaches using different correlation functions $\zeta(t)$ to obtain a temperature dependent signal

$$\hat{S} = \int_0^{t_S} \mathrm{d}t \, e^{-e_\nu(T,E_T,\sigma_\nu)t}\zeta(t) \quad (2)$$

are all based on simplifying assumptions which limit the usability of the analytical expression [2]–[5]. These limitations are easily overcome when the DLTS simulations are obtained with an advanced device simulation tool [6]. The transient relaxation of a device after an abrupt change in the applied bias is simulated which has the following advantages:

1) Instead of only thermal emission into one band e_ν all coupling processes (e_n, e_p, c_n, c_p) of the trap to all bands are evaluated.
2) Instead of homogeneous distributions an actual process-related and spatially resolved defect profile is used.
3) The occupation of defect levels is computed consistently with the position of the Fermi level.

In order to explain the broadening of DLTS spectra a coupling of different energy levels is implemented instead of just integrating over a distribution of independent energy levels,

$$\begin{aligned} \frac{\mathrm{d}n_i}{\mathrm{d}t} &= e_{p,i}(N_i - n_i) - e_{n,i}n_i \quad (3)\\ &+ c_{12,i}(N_i - n_i)n_{i+1} - e_{12,i}(N_{i+1} - n_{i+1})n_i \\ &- c_{12,i-1}(N_{i-1} - n_{i-1})n_i \\ &+ e_{12,i-1}(N_i - n_i)n_{i-1} \ . \end{aligned}$$

The set of coupled differential equations (3) resulting from the model in Fig. 1 is integrated numerically with a symplectic integrator to directly obtain a DLTS signal. This formalism is easily extended to N levels where only the neighboring levels are coupled to each other. Corresponding results of this numerical integration are compared in Figs. 4 and 5.

Results

The solution of the system (3) yields a substantial broadening of the DLTS signal as can be seen from Fig. 4 and, therefore, seems to represent a suitable model to explain very broad DLTS peaks. It differs from the S-Device simulation result where a uniform distribution of independent defect levels within an energy interval $E = E_C - 0.35\mathrm{eV} \pm 0.15\mathrm{eV}$ was assumed. The low-temperature tail of this peak was neither reproduced by the numerically integrated result nor by the S-Device simulation of the DLTS signal. This is probably because another level is present in the sample which cannot be resolved as a distinct peak in the DLTS measurement. Despite the use of simulated defect profiles, the amplitude of the DLTS peak, which is (beside other dependencies) directly proportional to the concentration of electrically active defects, is still a fitting parameter. It is not possible to predict the extent of decoration of the dislocation loops with other point-like impurities [8]. Hence, the concentration of peripheral interstitials in the dislocation loops can be deemed as an approximation to the maximum concentration of active defects. (see Fig. 3).

978-3-901578-26-7

ACKNOWLEDGEMENT

The research leading to these results has received funding from the European Seventh Framework Program FP7/2007-2013) under the grant agreement No. 258547 (ATEMOX).

REFERENCES

[1] D.V.. Lang , J. Appl. Phys., Vol. 45, No. 7, Jul. 7, 1974, pp. 3023 - 3032.

[2] C. Hardalov et al. and K Kirov et al., J. Appl. Phys., Vol. 71, No. 5, Mar. 1, 1992, pp. 2270 - 2273.

[3] A. Das and V.A. Singh and D.V. Lang, Semicond. Sci. Technol., Vol. 3, 1988, pp. 1177 - 1183.

[4] G.L. Miller and J.V. Ramirez and D.A.H. Robinson, J. Appl. Phys., Vol. 46, No. 6, Jun. 1975, pp. 2638 - 2644.

[5] A.A. Istrativ and O.F. Vyvenko and H. Hieslmair and E.R. Weber, Meas. Sci. Technol., Vol. 9, 1998, pp. 477 - 484.

[6] Synopsys Inc, Sentaurus Device User Guide, version F- 2011.09

[7] A. Schenk and U. Krumbein, J. Appl. Phys., Vol. 78, No. 5, Sep. 1, 1995, pp. 3185 - 3192.

[8] V. Moroz and M. Choi, ECS Trans. Vol. 33, No. 11m 2010, pp. 221-236.

[9] Private communications within the ATEMOX project. www.atemox.eu

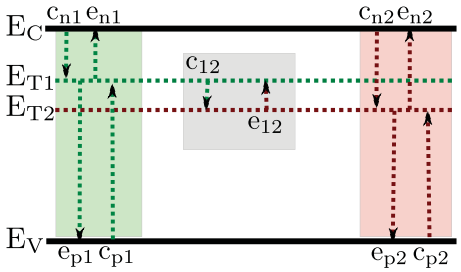

Fig. 1. Schematic representation of two defect levels (E_{t1} and E_{t2}) in the band gap. Each defect level couples to conduction and valence band. Furthermore, an inter-level coupling is represented by the coupling constants c_{12} and e_{12}. This model of the coupling of two defect levels from [7] is available in the commercial device simulator S-Device.

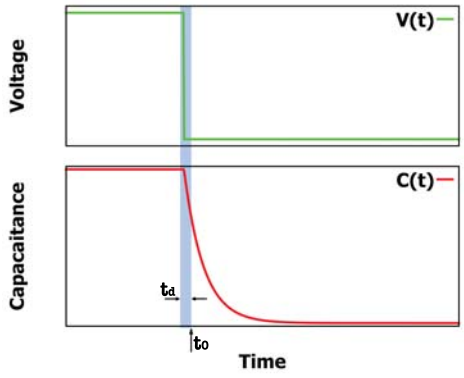

Fig. 2. Relation between voltage pulse configuration $V(t)$ and measured capacitance transient signal $C(t)$. A thorough description and analysis of the experimental setup can be found in [1]. Here t_d depicts the typical downtime of the instrumentation after the abrupt voltage change which leads to an overshoot in the detection hardware and hence a downtime which offsets the first measured point relative to the actual zero point of the switching process. For the device simulation C(t) curves are simulated for every temperature point. Script-based extraction of the necessary information from the simulation files is conducted to construct a DLTS signal.

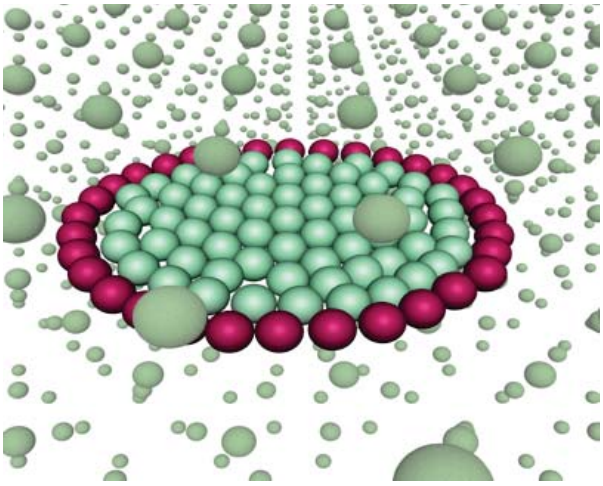

Fig. 3. Schematic visualization of the model for electrically active defects (red) in a dislocation loop.

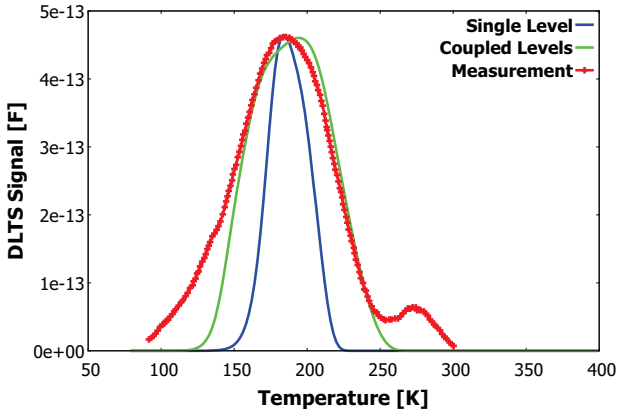

Fig. 4. Comparison of measured DLTS signal (red curve) [9] with numerically integrated signals for the single defect level (blue curve) and an ensemble of defect levels distributed over an interval of $\pm 0.15eV$ around the energy value $E_0 = E_C - 0.35eV$. (green curve) This energy interval is descretized into 15 smaller intervals and each of them is assigned to a normalized trap population. Energetic neighbouring populations are coupled to each other as demonstrated in Eq. (3).

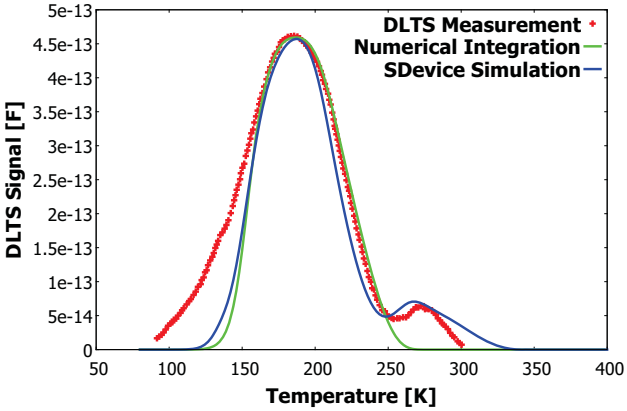

Fig. 5. Measured DLTS signal (red curve), numerically computed DLTS signal with parameters identical to those listed in the caption of Fig. 4. The blue line shows the S-Device simulation with the same energy distribution as used for the numerical solution. The defect levels in this device simulation are assumed to be independent.